

# An EGSnrc investigation of cavity theory for ion chambers measuring air kerma

Lesley A. Buckley,<sup>a)</sup> I. Kawrakow, and D. W. O. Rogers

*Ionizing Radiation Standards, National Research Council of Canada, Ottawa K1A 0R6, Canada*

(Received 20 December 2002; accepted for publication 24 March 2003; published 30 May 2003)

The EGSnrc system is used to compare the response of an aluminum-walled thimble chamber to that of a graphite-walled thimble chamber for a  $^{60}\text{Co}$  beam. When compared to previous experimental results, the EGSnrc values of the ratios of chamber response differ by as much as 0.7% from the experiment. However, it is shown that this difference can be more than accounted for by switching from using the graphite mean excitation energy of 78 eV used in dosimetry protocols to the value of 86.8 eV suggested by more recent stopping-power experiments. This suggests that the uncertainty analysis of Monte Carlo results must be done more carefully, by taking into account uncertainties in the underlying basic data such as the electron and photon cross sections. In comparison to Spencer–Attix cavity theory for a thick-walled ion chamber, the Monte Carlo calculated values of the chamber response differ from the expected ones by 0.15% and 0.01% for the graphite and aluminum chambers, respectively, which are comparable to previously reported values for the Spencer–Attix correction factors. EGSnrc is also used to investigate the effect on the chamber response of thin dag layers on the inside of the aluminum wall. There is good agreement between the calculated and measured changes in chamber response versus the thickness of the dag. The results are compared to the predictions of the Almond–Svensson extension of cavity theory and show that the theory does not correctly predict the chamber response in the presence of thin dag layers. This finding is in agreement with previously reported experimental results. It is demonstrated that the values of  $\alpha$ , the fraction of ionizations in the gas arising from electrons generated in the dag layer, used in the theory, are not the source of the disagreement.

[DOI: 10.1118/1.1573891]

Key words: dosimetry, Monte Carlo, ionization chamber

## I. INTRODUCTION

Spencer–Attix cavity theory is the basis of modern dosimetry protocols<sup>1–3</sup> and, as applied to thick-walled ion chambers, is also the basis of primary standards of air-kerma in  $^{60}\text{Co}$  beams.<sup>4</sup> The Almond–Svensson extension of cavity theory is frequently used when dealing with chamber walls having two components.<sup>5</sup> Monte Carlo calculations are used extensively in dosimetry protocols and in the determination of a wide variety of correction factors in radiation dosimetry. The recently developed EGSnrc Monte Carlo code<sup>6,7</sup> is the first Monte Carlo code thought to be able to simulate ion chamber response at the 0.1% level of accuracy, at least with respect to its own cross sections.<sup>8</sup>

In the 1980's, Nahum *et al.*<sup>9</sup> reported some interesting measurements which were a test of cavity theory, of the Almond–Svensson extension of cavity theory, and of Monte Carlo simulations. The measurements were performed using an ion chamber with two thimbles, one graphite and one aluminum, for which the volumes were known independently. The relative response of these two chambers in a  $^{60}\text{Co}$  beam was measured, as well as the response of the aluminum-walled chamber relative to that of the graphite-walled chamber as thin layers of graphite dag were added to the interior wall of the aluminum chamber. As a result of the measurements, Nahum *et al.* reported reasonable agreement between the measured and predicted ratios of responses for the pure-walled chambers. However, the measured responses

as a function of the thickness of the dag layer could not be explained either by the Almond–Svensson predictions or by some unpublished Monte Carlo calculations performed using EGS4.

In view of the much more accurate Monte Carlo code available today, and the higher statistical precision which can be obtained, it is worthwhile to re-investigate these experimental measurements. The EGSnrc user-code CAVRZnrc<sup>10</sup> is used to compare the response of an aluminum-walled thimble chamber to that of a graphite-walled chamber. Upon comparison of the Monte Carlo results to the experimental measurements, it becomes evident that the experimental measurements of Nahum *et al.* provide one of the relatively rare, high-precision examples in which the agreement between experiment and calculations depends on a knowledge of the absolute values of the electron and photon cross sections used in the calculations. This dependence is used to study the implications of the uncertainty in the mean excitation energy on the determination of the stopping power for graphite. The mean excitation energy plays a key role in the value of the primary standards of air-kerma in  $^{60}\text{Co}$  beams. In addition to comparing the measured ratios of the ion chamber responses to the ratios calculated using CAVRZnrc, they are also compared to the values predicted by cavity theory. The EGSnrc-calculated ion chamber responses are also used to compute the magnitude of any correction to the Spencer–Attix cavity theory,  $K_{SA}$ , as introduced by Borg *et al.*<sup>11</sup>

The CAVRZnrc code is also used to investigate the effects on the calculated response of adding thin layers of dag to the inside of the aluminum chamber wall. In comparison to the experimental values, the calculated responses once again provide a demonstration of the need for further investigation of the mean excitation energy of graphite. The calculated responses are also used to study the accuracy of the Almond–Svensson extension of cavity theory.

## II. METHODS

### II. A. Cavity theory

Spencer–Attix cavity theory, applied to thick-walled, air-filled ion chambers, predicts that the air kerma free in air,  $K_{\text{air}}$ , at the location of the center of an ion chamber, in the absence of the chamber, is given by<sup>12</sup>

$$K_{\text{air}} = D_{\text{air}} \left( \frac{\bar{L}}{\rho} \right)_{\text{air}}^{\text{wall}} \left( \frac{\bar{\mu}_{\text{en}}}{\rho} \right)_{\text{air}}^{\text{wall}} \frac{1}{(1 - \bar{g}_{\text{air}})} K, \quad (1)$$

where  $(\bar{\mu}_{\text{en}}/\rho)_{\text{wall}}^{\text{air}}$  is the average ratio of mass energy absorption coefficients in the air and wall material,  $\bar{g}$  is the average fraction of the electron's energy that is lost in the air via radiative processes,  $D_{\text{air}}$  is the dose to the air in the cavity, and  $(\bar{L}/\rho)_{\text{air}}^{\text{wall}}$  is the stopping-power ratio. The correction factor,  $K$ , includes a correction for attenuation and scatter in the chamber wall ( $K_{\text{wall}}$ ), an axial non-uniformity correction which accounts for any divergence in the beam ( $K_{\text{an}}$ ), and an electrode correction which accounts for a change in the ionization in the chamber due to a change in electrode material ( $K_{\text{el}}$ ). In this study,  $K_{\text{an}}$  is unity since all calculations were performed using a parallel beam incident on the chamber and in any case would be very close to unity for calculations for a point source at 100 cm from a Farmer-type chamber as discussed by Bielajew and Rogers.<sup>13</sup>

Deviations from Spencer–Attix cavity theory for thick-walled ion chambers, as formulated above, can be accounted for by the introduction of another correction factor,  $K_{\text{SA}}$ , into Eq. (1). The Spencer–Attix correction factor can be computed using the EGSnrc system and is given by:<sup>11</sup>

$$K_{\text{SA}} = \frac{K_{\text{air}}(1 - \bar{g}_{\text{air}})}{D_{\text{air}} \left( \frac{\bar{L}}{\rho} \right)_{\text{air}}^{\text{wall}} \left( \frac{\bar{\mu}_{\text{en}}}{\rho} \right)_{\text{air}}^{\text{wall}} K_{\text{wall}}} = \frac{K_w(1 - \bar{g}_{\text{wall}})}{D_{\text{air}} \left( \frac{\bar{L}}{\rho} \right)_{\text{air}}^{\text{wall}} K_{\text{wall}}}, \quad (2)$$

where  $K_w$  is the kerma in the wall material and the other symbols are as described earlier. Equation (2) only applies if the chamber is made of a single material.

For a composite chamber wall, as in the case of a thin dag layer on the inside of an aluminum wall, the chamber response is predicted by the Almond–Svensson extension to cavity theory.<sup>5</sup> In this case the response of a composite chamber,  $D_{\text{air}}^{\text{Al}}$ , relative to that of a pure aluminum-walled chamber is given by

TABLE I. EGSnrc calculated values of restricted stopping-power ratios,  $(\bar{L}/\rho)_{\text{air}}^{\text{med}} (\Delta = AE-511 \text{ keV})$ , spectrum-averaged ratios of mass energy absorption coefficients,  $(\bar{\mu}_{\text{en}}/\rho)_{\text{med}}^{\text{air}}$ , and average radiative energy loss fraction,  $\bar{g}$ , for three values of the electron energy cutoff,  $AE$ . The stopping-power ratios were computed using a mean excitation energy for graphite of 78 eV and a density-effect correction computed for the bulk density of 1.7 g/cm<sup>3</sup>. All quantities were computed using a <sup>60</sup>Co spectrum described elsewhere (Ref. 21) and a photon energy cutoff,  $AP$ , of 1 keV. The statistical uncertainties in the stopping-power ratios are less than 0.009% and less than 0.02% and 0.03% for the ratio of mass energy absorption coefficients and  $\bar{g}$  values, respectively.

Medium	$AE$ (keV)	$(\bar{L}/\rho)_{\text{air}}^{\text{med}}$	$(\bar{\mu}_{\text{en}}/\rho)_{\text{med}}^{\text{air}}$	$\bar{g}$
Al	512	0.820 52	1.0400	0.005 95
	521	0.861 19	1.0373	0.005 94
	527	0.865 43	1.0373	0.005 93
Graphite	512	1.006 91	0.9990	0.002 59
	521	1.001 78	0.9992	0.002 55
	527	1.001 22	0.9993	0.002 54
Air	512	...	...	0.003 09
	521	...	...	0.003 07
	527	...	...	0.003 06

$$\frac{D_{\text{air}}^{\text{Al}}}{D_{\text{air}}^{\text{pure Al}}} = \frac{\left( \frac{\bar{L}}{\rho} \right)_{\text{air}}^{\text{Al}} \left( \frac{\bar{\mu}_{\text{en}}}{\rho} \right)_{\text{Al}}^{\text{air}}}{\alpha \left( \frac{\bar{L}}{\rho} \right)_{\text{air}}^{\text{gr}} \left( \frac{\bar{\mu}_{\text{en}}}{\rho} \right)_{\text{gr}}^{\text{air}} + (1 - \alpha) \left( \frac{\bar{L}}{\rho} \right)_{\text{air}}^{\text{Al}} \left( \frac{\bar{\mu}_{\text{en}}}{\rho} \right)_{\text{Al}}^{\text{air}}}, \quad (3)$$

where  $\alpha$  is the fraction of ionizations due to electrons created by photon interactions in the dag layer and  $(1 - \alpha)$  is the fraction of ionizations due to electrons created in the aluminum.

Using Eqs. (1) and (3) we obtain an expression for the ratio of the dose to the gas in the dag-coated, aluminum-walled chamber,  $D_{\text{air}}^{\text{Al}}$ , to that in the pure, graphite-walled chamber,  $D_{\text{air}}^{\text{gr}}$ :

$$\frac{D_{\text{air}}^{\text{Al}}}{D_{\text{air}}^{\text{gr}}} = \frac{K_{\text{wall}}^{\text{gr}} K_{\text{el}}^{\text{gr}}}{K_{\text{wall}}^{\text{Al}} 1} \frac{\left( \frac{\bar{L}}{\rho} \right)_{\text{air}}^{\text{gr}} \left( \frac{\bar{\mu}_{\text{en}}}{\rho} \right)_{\text{gr}}^{\text{air}}}{\alpha \left( \frac{\bar{L}}{\rho} \right)_{\text{air}}^{\text{gr}} \left( \frac{\bar{\mu}_{\text{en}}}{\rho} \right)_{\text{gr}}^{\text{air}} + (1 - \alpha) \left( \frac{\bar{L}}{\rho} \right)_{\text{air}}^{\text{Al}} \left( \frac{\bar{\mu}_{\text{en}}}{\rho} \right)_{\text{Al}}^{\text{air}}}. \quad (4)$$

All of the quantities in Eq. (4) have been calculated using the EGSnrc system. Table I summarizes the restricted stopping-power ratios, mass energy absorption coefficients and  $\bar{g}$  values calculated in this study for three values of the electron cutoff energy. Separate calculations show that the variation in  $\bar{g}$  is due to the change in ECUT along with  $AE$ , and not due to  $AE$  specifically. The average mass energy absorption coefficients are computed using a combination of two EGSnrc user-codes. The user-code  $g$  is used to compute the average fraction,  $\bar{g}$ , of the electron's energy lost by radiative processes by scoring all radiative losses as each charged particle slows down in an infinite medium and taking  $\bar{g}$  to be this quantity as a fraction of the total kinetic energy transferred to

charged particles. The user-code DOSRZnrc<sup>10</sup> is used to calculate the kerma in a given medium, per unit fluence,  $K_{\text{med}}/\Phi$ . The average mass energy absorption coefficient is then calculated from:

$$K_{\text{med}} = \Psi \left( \frac{\bar{\mu}_{\text{en}}}{\rho} \right)_{\text{med}} \frac{1}{(1 - \bar{g}_{\text{med}})}, \quad (5)$$

where  $\Psi$  is the energy fluence. A more detailed account of this sequence of calculations is given in a previous publication.<sup>11</sup>

### II. A. 1. Stopping power ratios

Spencer–Attix restricted, mass-collision stopping-power ratios are computed using the EGSnrc user-code SPRRZnrc<sup>10</sup> using the photon regeneration option as needed for free in air calculations. The material densities used in the calculations are 1.7 and 2.7 g/cm<sup>3</sup> for graphite and aluminum respectively and match the densities used in the modeling of the chamber geometries.

The value of the restricted stopping power is dependent on the choice of cutoff energy,  $\Delta$ , used in the calculations. The stopping-power ratios in Table I are shown for three values of the cutoff energy: 1 keV, for consistency with the other Monte Carlo calculated values in this paper, 10 and 16 keV. Traditionally, dosimetry protocols use a value of  $\Delta = 10$  keV for their stopping-power ratios.<sup>1</sup> In primary standards labs however,  $\Delta$  is typically dictated by chamber size. In the latter case,  $\Delta$  can be related to the lowest energy of electrons that can just cross the cavity. This is accomplished by computing the mean chord length given by  $l = 4V/S$  where  $V$  is the volume of the air in the cavity and  $S$  is the surface area of the cavity. The value of  $\Delta$  is then the electron energy for which the CSDA range is equal to the mean chord length. For the chamber being studied here, this implies  $\Delta = 16$  keV.

The stopping powers are computed from Bethe stopping-power theory which requires a knowledge of several quantities describing properties of the medium. One such quantity is the mean excitation energy,  $I$ , which is a weighted, geometric average of the excitation energies of the medium. The weighting factor depends on both the physical state and the electronic structure of the material. For many materials, it is necessary to determine the mean excitation energy from experimental data. In the case of graphite, ICRU Report 37<sup>14</sup> uses a value of  $I = (78 \pm 7)$  eV, based on experimental data for proton stopping powers at high energies. More recent experiments<sup>15</sup> yield much lower uncertainty on  $I$  and suggest a value of  $I = (86.9 \pm 1.2)$  eV for graphite. In this study, the stopping powers for graphite are computed for both values of  $I$  and the results from the two cases are compared.

The stopping powers are also sensitive to the density-effect correction used in the calculation. As a charged particle moves within a medium it causes the polarization of atoms in the medium, which in turn decreases the electromagnetic field acting on the particle, thereby reducing the stopping power. This effect is more evident in dense materials and has a greater impact on the stopping power at high

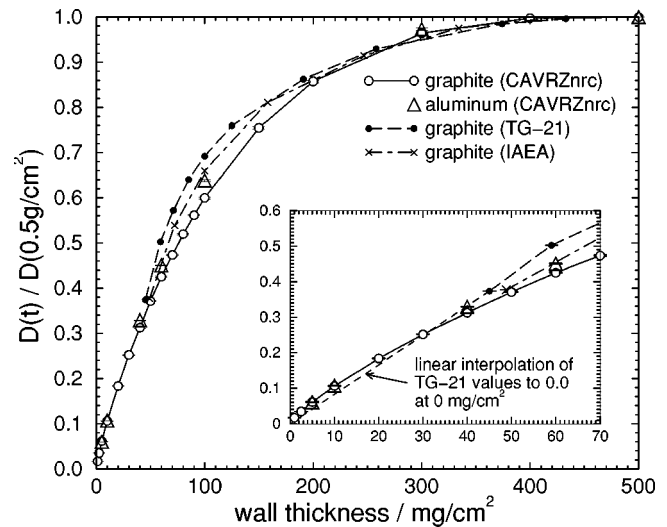


FIG. 1. Ratio of dose to the cavity for a thin-walled graphite chamber relative to a chamber with full build-up as a function of wall thickness,  $t$ , as computed using CAVRZnrc for a <sup>60</sup>Co beam. The calculated values are shown in comparison to the published values of  $\alpha$  from the AAPM TG-21 code of practice—Ref. 1 (which are also used in the TG-51 protocol—Ref. 2) and the IAEA protocol (Ref. 18). The points from each of the protocols were obtained through digitization of figures within the reports showing the value of  $\alpha$  as a function of wall thickness. The open triangles were computed for an aluminum-walled chamber. The insert shows the region below 70 mg/cm<sup>2</sup> and includes the linear interpolation of the TG-21 values to 0.0 at 0 mg/cm<sup>2</sup>. The axes on the insert are the same as on the main graph.

energies. The calculations involving the aluminum chamber use the density-effect corrections from ICRU Report 37<sup>14</sup> based on a density of 2.7 g/cm<sup>3</sup>. In the case of graphite, which is a porous and highly inhomogeneous material, the bulk density of 1.7 g/cm<sup>3</sup> used in ICRU Report 37 differs significantly from the grain density of 2.265 g/cm<sup>3</sup>. It is not obvious which value of the density correction should be used since the theory is intended for homogeneous media, however recent experimental evidence supports the use of the grain density (2.265 g/cm<sup>3</sup>) when computing the density effect.<sup>16,17</sup> The implications of the uncertainty in the graphite density effect, as they relate to the Monte Carlo results, will be discussed in a subsequent section.

### II. A. 2. $\alpha$ values

As seen from Eq. (4), the theoretical value of  $D_{\text{air}}^{\text{Al}}/D_{\text{air}}^{\text{gr}}$  is dependent on the value of  $\alpha$ , the fraction of ionizations from electrons created by photon interactions in the dag layer. For the purposes of this study, the values for  $\alpha$  are computed using the CAVRZnrc user-code. For a dag layer of thickness  $t$ ,  $\alpha$  is given by the ratio of the dose to the air in a graphite chamber of wall thickness  $t$  to the dose to the air in a graphite chamber with full build up. The calculations use a pure-graphite wall and the electrode is replaced with air to eliminate the contribution of ionizations from the electrode for thin walls. Figure 1 shows the values of  $\alpha$  calculated using CAVRZnrc in comparison with the values given by the AAPM TG-21 protocol<sup>1</sup> and by the IAEA TRS-277 Code of Practice for absorbed dose determination.<sup>18</sup> The points from

the AAPM and IAEA curves were obtained from Figs. 1 and 15 in the respective reports, both of which base their data on the work of Lempert *et al.*<sup>19</sup>

Figure 1 shows significant discrepancies, for some wall thicknesses, between values of  $\alpha$  from the different sources. For wall thicknesses between 50 and 150 mg/cm<sup>2</sup>, the largest variation in  $\alpha$  values occurs for a wall thickness of 100 mg/cm<sup>2</sup>, which shows differences between the CAVRZnrc values and the AAPM and IAEA values of 15% and 10%, respectively. However, these result in differences of only 1.1% and 0.7%, respectively, when computing the ratio of chamber responses given by Eq. (4) for  $\Delta = 16$  keV. If we consider instead, a wall thickness more typical of ion chambers used in dosimetry, we find that at a wall thickness of 65 mg/cm<sup>2</sup>, the effect of the variation in  $\alpha$  on the calculated ratio of chamber responses is no greater than 1% for either the AAPM or IAEA values, when compared to using the CAVRZnrc values of  $\alpha$ . Furthermore, we may consider a more commonly used chamber, such as the NE2571 chamber used in water, as is typically used in TG-51 calibrations, and can compute the value of  $P_{\text{wall}}$ , which corrects for the fact that the chamber wall and the dosimetry phantom are of different materials. The NE2571 chamber has a graphite wall, 0.065 g/cm<sup>2</sup> thick. In this case, the values of  $P_{\text{wall}}$  computed using the three sources of  $\alpha$  values discussed here, agree to within 0.17% in all cases.

In dosimetry protocols, the value of  $\alpha$  is treated as being independent of the chamber wall composition, provided the wall is made from low atomic number materials. Figure 1 shows calculated values of  $\alpha$  for both graphite and aluminum walls. Since aluminum is an extreme case and differs significantly from graphite in atomic number, the agreement between the graphite and aluminum values justifies the use of material-independent  $\alpha$  values for low atomic number materials.

Neither the AAPM nor the IAEA protocol gives  $\alpha$  values for chamber-wall thicknesses below 45 mg/cm<sup>2</sup>. In the case of thin dag layers, it is common for dosimetry calculations to assume a linear interpolation to  $\alpha = 0$  at a wall thickness of 0 mg/cm<sup>2</sup>.<sup>20</sup> The insert in Fig. 1 shows the  $\alpha$  values for wall thicknesses below 70 mg/cm<sup>2</sup> and indicates the linear interpolation of the AAPM values to  $\alpha = 0$  at 0 mg/cm<sup>2</sup>. In the region of the linear interpolation, interpolated values of  $\alpha$  differ by as much as 22% from the calculated values, however the potential effect on the predicted value of  $D_{\text{air}}^{\text{Al}}/D_{\text{air}}^{\text{gr}}$ , using Eq. (4), is less than 0.3%.

## II. B. Ion chamber calculations

The ion chamber calculations are based upon the experimental geometry used by Nahum *et al.*<sup>9</sup> The thimble chamber has a 1 mm aluminum central electrode and an inner cavity length of 2 cm. In accordance with the experimental geometry, the inner diameter of the thimble is 3.15 mm for the graphite thimble and 3.41 mm for the aluminum thimble. The thimble wall thicknesses are 0.35 and 0.09 mm for the graphite and aluminum chambers respectively, resulting in identical outer dimensions for the two thimbles. Experimen-

tally, build-up caps were used to achieve electronic equilibrium in a <sup>60</sup>Co beam, which in the calculations is achieved using a 0.5 g/cm<sup>2</sup> total wall thickness. The build-up caps were such that they could be used with either of the two thimbles. A thin layer of dag on the inside of the aluminum wall is varied between 1 and 150 mg/cm<sup>2</sup> thick. The composition of the dag is 87.48% graphite, 3.00% hydrogen, and 9.52% oxygen and is identical to that of the Dag 154 used in the experiment. The material densities are 1.7 and 2.7 g/cm<sup>3</sup> for the graphite and aluminum, respectively, and the dag layer has a density of 0.93 g/cm<sup>3</sup>. The experimental uncertainty on the density of the dag layer was 0.02 g/cm<sup>3</sup>. A <sup>60</sup>Co beam is incident on the chamber from the side. The <sup>60</sup>Co spectrum is taken from a previously reported<sup>21</sup> simulation of the <sup>60</sup>Co therapy machine used for the experiments. All calculations are performed for an ion chamber in air.

The EGSnrc user-code CAVRZnrc<sup>10</sup> is used to compute the absorbed dose to the cavity,  $D_{\text{air}}$ , and the correction factor for wall attenuation and scatter,  $K_{\text{wall}}$ . This correction accounts for a decrease in the response of the chamber due to attenuation of primary photons in the wall and an increase in response due to photons scattered in the walls.

The calculations are performed using a photon splitting technique<sup>10,22</sup> that increases the efficiency of typical ion chamber calculations by a factor of 5 compared to using photon interaction forcing. Unless otherwise stated, the following settings apply to all calculations:  $AP = 1$  keV,  $AE = 512$  keV, spin effects in the multiple scattering are off and the photon splitting factor is 130. The effect of turning the spin off for these calculations is less than 0.1%. The energy cutoff of  $AE = 512$  keV is chosen based on a previous study<sup>23</sup> which showed that the dose to the air changes slightly as the cutoff energy is increased but is constant for cutoff energies below 513 keV. For the chamber being studied here, the dose to the air increases by 0.2% and 0.03% in changing from  $AE = 512$  keV to  $AE = 521$  keV for the aluminum and graphite thimbles, respectively. The CPU time required to achieve statistical uncertainties on the order of 0.08% is 6 h on a 1.5 GHz machine.

## II. C. Experimental data

For a meaningful comparison with the present EGSnrc results, the experimental results of Nahum *et al.*<sup>9</sup> require certain corrections to be applied. Table I in the paper by Nahum *et al.* cites ratios of mass ionization for a variety of chambers. These ratios were obtained from the raw experimental data by applying three correction factors: one for the attenuation and scatter in the aluminum and graphite walls, one for the presence of impurities in the aluminum and one for the effect of having an aluminum central electrode instead of a graphite electrode in the graphite-walled chamber. The first correction is the ratio of the scatter and attenuation corrections in the aluminum and graphite walls. This corresponds to a ratio of  $K_{\text{wall}}$  values for the two chambers. Nahum *et al.* report this correction to be  $1.0008 \pm 0.0011$ . For unexplained reasons, this differs by almost 0.4% from the ratio of values calculated using CAVRZnrc ( $K_{\text{wall}}^{\text{gr}}/K_{\text{wall}}^{\text{Al}} = 0.9969$

$\pm 0.01\%$ ), although this difference is not critical since we only use the value of Nahum *et al.* to determine their uncorrected values. When correcting the raw data values to obtain the values reported in the paper by Nahum *et al.*, the raw data values are divided by their scattering and attenuation correction. For the second correction, Nahum *et al.* estimated that impurities in the aluminum increased the reading in the aluminum-walled chamber by  $0.19 \pm 0.08\%$ . This corresponds to a correction factor of  $1/1.0019$  when correcting the raw data value. The third correction accounts for the increase in the measured ionization in the graphite chamber due to the collecting electrode being aluminum rather than graphite. Nahum *et al.* report this correction to be  $(0.9 \pm 0.2)\%$ . A calculation of this effect using CAVRZnrc results in a value of  $(0.63 \pm 0.11)\%$  which agrees with another previous, EGS4/PRESTA Monte Carlo calculation that gave a value of  $(0.58 \pm 0.13)\%$ <sup>24</sup> and the measured result of Palm and Mattsson of  $(0.8 \pm 0.2)\%$ .<sup>25</sup>

Comparison of the calculations using CAVRZnrc with the experimental results does not require that all three corrections be applied. The central electrode correction is not included since, as in the case of the raw experimental data, all of the Monte Carlo calculations are performed using an aluminum central electrode in both chambers. The correction for the impurities in the aluminum however, must be applied to the raw experimental data since the Monte Carlo calculations are for an idealized chamber with pure aluminum. Therefore all subsequent experimental values cited in this paper include the impurity correction. All of the experimental raw data values and their uncertainties have been obtained by digitization of Fig. 1 in the paper by Nahum *et al.*

### III. RESULTS

#### III. A. Chambers with walls of one material

The first set of experimental measurements by Nahum *et al.*<sup>9</sup> compared the response in an aluminum-walled chamber to that in a graphite-walled chamber. Correcting only for the impurities in the aluminum, Nahum *et al.* report the relative mass ionization in the two chambers to be  $1.094 \pm 0.003$ . This differs by 0.7% from the CAVRZnrc calculated value of  $D_{\text{gas}}^{\text{Al}}/D_{\text{gas}}^{\text{gr}} = 1.1024 \pm 0.0004$ , which was computed for a mean excitation energy of 78 eV for graphite. If, however, we use a mean excitation energy of 86.8 eV as suggested by Bichsel *et al.*,<sup>15</sup> the calculated dose ratio becomes  $1.0890 \pm 0.0004$ , 0.5% lower than the experimental value of Nahum *et al.* These results are summarized in Table II. Although neither calculated value agrees with the experimental value, it is interesting to note that the experimental ratio falls in between the two CAVRZnrc values computed for different  $I$  values of graphite. This suggests that the discrepancy between the Monte Carlo and the experiment may be accounted for, at least in part, by lack of knowledge of the correct stopping powers.

In addition to the value of  $I$ , the uncertainty in the knowledge of the stopping powers also stems from the density of graphite used to evaluate the density-effect correction. The two CAVRZnrc dose ratios reported earlier,  $1.1024 \pm 0.0004$

TABLE II. Comparison of  $D_{\text{air}}^{\text{Al}}/D_{\text{air}}^{\text{gr}}$  values from the experimental data of Nahum *et al.* (Ref. 9), CAVRZnrc calculations, and from the predictions of Spencer–Attix cavity theory, given by Eq. (4) for  $\alpha=0$ ,  $K_{\text{el}}=1.0063$ , and  $K_{\text{wall}}^{\text{gr}}/K_{\text{wall}}^{\text{Al}}=0.9969$  for two values of the energy cutoff,  $\Delta$ . The ratio of the  $K_{\text{wall}}$  values was constant for all values of  $AE$  used in the calculations. The experimental data have been corrected for impurities in the aluminum and the CAVRZnrc values were computed using a density correction for a graphite density of  $1.7 \text{ g/cm}^3$  and a mean excitation energy for graphite of 78 eV (except where otherwise stated).

Source of dose ratio	$D_{\text{air}}^{\text{Al}}/D_{\text{air}}^{\text{gr}}$
Nahum <i>et al.</i>	$1.094 \pm 0.003$
CAVRZnrc ( $I=78 \text{ eV}$ )	$1.1024 \pm 0.0004$
CAVRZnrc ( $I=86.8 \text{ eV}$ )	$1.0890 \pm 0.0004$
SA theory ( $\Delta=10 \text{ keV}$ )	1.1100
SA theory ( $\Delta=16 \text{ keV}$ )	1.1041

and  $1.0890 \pm 0.0004$ , for  $I=78 \text{ eV}$  and  $I=86.8 \text{ eV}$ , respectively, were both computed using a graphite density of  $1.7 \text{ g/cm}^3$  for the density-effect correction. If these two ratios are computed using a density of  $2.265 \text{ g/cm}^3$  instead, they become  $1.1017 \pm 0.0004$  and  $1.0870 \pm 0.0004$ , respectively. In both cases, the effect of using one density effect in place of the other is less than 0.2%.

The calculated ratio of chamber responses is proportional to the ratio of the aluminum and graphite photon cross sections, and therefore the uncertainty in the calculations is also affected by the uncertainties in these cross sections. In the energy region dominated by the Compton interaction, the uncertainties in the photon cross sections are estimated to be about 1%.<sup>26–28</sup> However, for the range of energies most significant in a  $^{60}\text{Co}$  beam, it is likely that the uncertainties, and especially the uncertainties related to ratios of photon cross sections, are less than 1%.<sup>23</sup>

It is also instructive to compare the CAVRZnrc results for the ratio of responses to the predictions of Spencer–Attix cavity theory, given by Eq. (4), for an  $\alpha$  value of 0. For a pure aluminum-walled chamber, this equation predicts dose ratios of 1.1100 and 1.1041 for energy cutoffs of 10 and 16 keV, respectively. These values, also shown in Table II, were computed using a mean excitation energy of 78 eV for graphite and should therefore be compared to the CAVRZnrc dose ratio of  $1.1024 \pm 0.0004$  reported earlier in this paper. Discrepancies between the calculated dose ratio and that predicted by cavity theory should be accounted for by ratios of the Spencer–Attix correction factors,  $K_{\text{SA}}$ , for graphite and aluminum, given by Eq. (2). Table III lists the values of  $K_{\text{SA}}$

TABLE III. EGSnrc calculated values of the Spencer–Attix correction factor,  $K_{\text{SA}}$ , for the aluminum-walled and graphite-walled thimble chambers for two values of the restricted stopping power cutoff energy,  $\Delta$ . A cutoff energy of  $\Delta=10 \text{ keV}$  is the commonly used value in dosimetry studies and  $\Delta=16 \text{ keV}$  is the chamber-specific value computed from the mean chord length of the cavity. The calculations are for a mean excitation energy,  $I$ , of 78 eV for graphite.

$\Delta$ (keV)	$K_{\text{SA}}^{\text{Al}}$	$K_{\text{SA}}^{\text{gr}}$
10	$1.0050 \pm 0.0003$	$0.9980 \pm 0.0003$
16	$1.0001 \pm 0.0003$	$0.9985 \pm 0.0003$

TABLE IV. Values of  $D_{\text{air}}^{\text{comp}}/D_{\text{air}}^{\text{gr}}$  for different combinations of thimble and cap material. The experimental values are taken from Nahum *et al.* (Ref. 9) and include a correction for impurities in the aluminum. The Monte Carlo values were computed using the user-code CAVRZnrc with a cutoff energy of 512 keV. For the graphite chamber, the calculations used a mean excitation energy,  $I$ , of 78 eV and a density-effect correction for a density of  $1.7 \text{ g/cm}^3$  in the graphite wall.

Thimble	Cap	Dose ratio (Nahum <i>et al.</i> )	Dose ratio (CAVRZnrc)	Difference
gr	gr	1.000	1.0000	...
gr	Al	$1.009 \pm 0.004$	$1.0161 \pm 0.0004$	+0.7%
Al	Al	$1.094 \pm 0.003$	$1.1024 \pm 0.0004$	+0.7%
Al	gr	$1.065 \pm 0.005$	$1.0656 \pm 0.0004$	+0.06%

computed for the two values of  $\Delta$  relevant to dosimetry calculations. Multiplication of the ratio of the  $K_{\text{SA}}$  values for the two chambers with the calculated CAVRZnrc dose ratio from Table II shows that the Spencer–Attix correction factor does (as it must, by definition) account for the difference between the CAVRZnrc result and the prediction of the Spencer–Attix theory as formulated in Eq. (1).

From the values in Table III, it is clear that the chamber-specific value of  $\Delta$ , 16 keV, provides better agreement between the theory and calculated results. This is consistent with the results of Borg *et al.*<sup>11</sup> and Mainegra-Hing *et al.*<sup>23</sup> This is particularly evident for the aluminum chamber, where the correction at  $\Delta = 10 \text{ keV}$  is 0.5% whereas it is less than 0.01% for a  $\Delta$  value of 16 keV. In the case of the graphite chamber, the correction to the theory is no more than 0.4% for either value of  $\Delta$ .

**III. B. Composite-walled chambers**

The paper by Nahum *et al.* also considers a variety of cases where the chamber wall is composed of two materials. In the first such set of measurements, Nahum *et al.* report relative mass ionization ratios for the aluminum chamber with a graphite cap and for the graphite chamber with an aluminum cap. Although the cap thicknesses were not stated explicitly in the experimental report, it is assumed for the calculations that the caps were thick enough to provide full buildup of  $0.5 \text{ g/cm}^2$  for each of the chambers, when used with their matching thimble. The experimental values are shown in Table IV along with the values of  $D_{\text{air}}^{\text{comp}}/D_{\text{air}}^{\text{gr}}$  calculated using CAVRZnrc, where  $D_{\text{air}}^{\text{comp}}$  is the dose to the air in the composite-walled chamber. The experimental values have been corrected for impurities in the aluminum. In no case does the CAVRZnrc dose ratio differ by more than 0.7% from the dose ratio determined by Nahum *et al.* As before, this discrepancy can be more than accounted for by uncertainty in the stopping powers.

The composite-wall experimental results of Nahum *et al.* also compare the response of an aluminum-walled chamber, lined with a thin layer of dag, to the response in a graphite-walled chamber. The experimental results, corrected for impurities in the aluminum, are shown in Fig. 2 along with the results calculated using CAVRZnrc. The CAVRZnrc results are computed using the ICRU Report 37 value for the mean

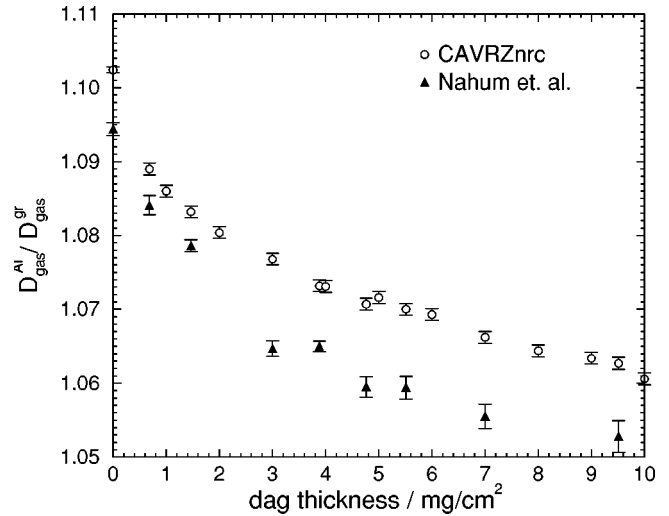


FIG. 2. The absorbed dose to the cavity for an aluminum-walled thimble chamber relative to that in a graphite-walled chamber for different thicknesses of dag in a  $^{60}\text{Co}$  beam. The open circles show the CAVRZnrc calculations with  $AE=512 \text{ keV}$  and the closed triangles show the raw data from Nahum *et al.*, corrected for impurities in the aluminum. Details of the corrections applied to the raw experimental data are described in the text. The CAVRZnrc calculations were performed using a mean excitation energy of 78 eV and a density-effect correction of  $1.7 \text{ g/cm}^3$  for the graphite wall.

excitation energy of graphite and used a graphite density of  $1.7 \text{ g/cm}^3$  to compute the density-effect correction. The density-effect correction for the dag layer is computed using a density of  $0.93 \text{ g/cm}^3$ .

The experimental results of Nahum *et al.* do not agree particularly well with the output from CAVRZnrc. However, when the CAVRZnrc results are normalized to the experimental data as in Fig. 3, the two sets of values show similar, but not identical, behavior as a function of dag thickness. The normalized CAVRZnrc values show a root mean square deviation of 0.0029 from the experimental values.

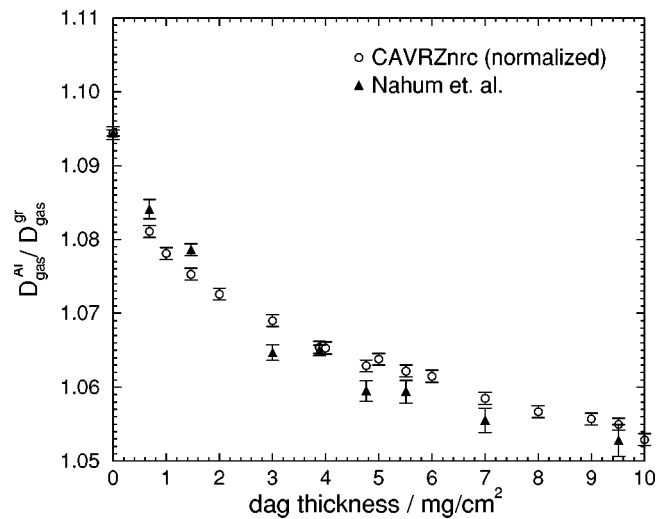


FIG. 3. As in Fig. 2, except that the CAVRZnrc results have been normalized to the experimental values for comparison of the overall shape of the two sets of values. The two curves show a root mean square deviation of 0.0029.

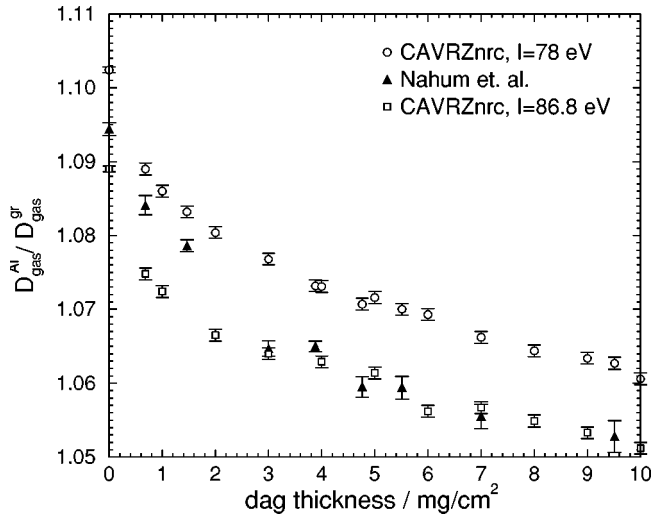


FIG. 4. The effect of changing the mean excitation energy,  $I$ , of graphite, on the relative dose ratio. The experimental data are shown as the closed triangles for comparison. All CAVRZnrc results were computed using  $AE = 512$  keV and used a density of  $1.70$  g/cm<sup>3</sup> for the density-effect correction in the graphite wall.

We may also once again consider the effect of using different values of the mean excitation energy on the calculated results. As shown in Fig. 4, if the chamber responses are computed for  $I = 86.8$  eV, the ratios of chamber responses are shifted from the previous values computed using  $I = 78$  eV. As in the case of the pure aluminum wall, the experimental dose ratios for the thin dag layers lie between the two curves calculated for the different  $I$  values.

It is also interesting to compare the CAVRZnrc results for the thin dag layers to the predictions of the Almond–Svensson extension of cavity theory. The theoretical curves

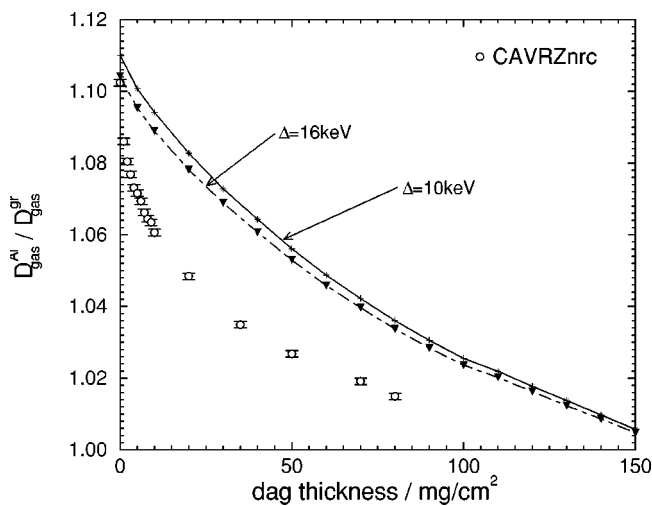


FIG. 5. The dose to the cavity for an aluminum-walled chamber with varying thicknesses of dag relative to that of a graphite-walled chamber. The lines show the behavior expected from the theory given by Eq. (4) for two values of  $\Delta$  and the open circles are the values calculated using CAVRZnrc with  $AE = 512$  keV and a mean excitation energy of graphite of 78 eV. The points indicated on the theory curves are the points at which the dose ratio was calculated using Eq. (4).

are shown in Fig. 5 for the two values of the restricted stopping power cutoff energy,  $\Delta$ , discussed earlier. Though the chamber specific value of  $\Delta$  gives values that are closer to the calculated ones, for thin dag layers, the output from the Monte Carlo calculation does not agree with the predictions of the Almond–Svensson formula for either value of  $\Delta$ . This agrees with the conclusion of Nahum *et al.*, who stated that the theory did not correctly predict the chamber response in the presence of thin dag layers. This finding is not surprising, given the very simple derivation of the Almond–Svensson formula, which ignores effects such as changes in the scattering power.

#### IV. CONCLUSIONS

The Monte Carlo code CAVRZnrc has been used to compute the ratio of the absorbed dose in an aluminum-walled thimble chamber to that in a graphite-walled chamber. The calculated ratio differs from a previously reported experimental value by 0.7%. This difference can be more than accounted for by changing the value of the mean excitation energy of graphite used to compute the stopping powers. This suggests the need for further investigation of the values of the mean excitation energy currently used in dosimetry protocols and primary standards in regard to more recent experimental values. The calculated response ratios vary by less than 0.2% when the density of the graphite used in the density-effect correction was changed from the bulk density to the grain density. The uncertainty in the calculated response ratios is also directly related to the uncertainty in the ratio of the photon cross sections. For the pure aluminum-walled chamber, the calculated dose ratio agrees with the predictions of Spencer–Attix cavity theory to within 0.06% when a chamber-specific value of the energy cutoff is used to determine the restricted stopping powers. If an energy cutoff of 10 keV is used, as is commonly done in dosimetry practice, this difference between the predicted value and the calculated result is 0.6%.

Calculations have also been performed for composite-walled chambers in relation to a pure graphite-walled chamber. For the case of an aluminum thimble with a graphite build-up cap and for a graphite thimble with an aluminum cap, the calculated chamber response ratios differ by up to 0.7% from the experiment. In the case of thin dag layers applied on the inside of an aluminum chamber wall, direct comparison of CAVRZnrc results and experiment shows that the calculated ratios of chamber response differ by less than 1% from the experimental values. Upon normalization to the experimental data, the Monte Carlo results show similar, but not identical behavior, with a root mean square deviation in the ratio of responses of 0.0029 from the experiment. The Almond–Svensson extension to cavity theory does not correctly predict the chamber response in the presence of the dag layers and it is demonstrated that the values of  $\alpha$  are not the source of the problem. Since the Almond–Svensson theory is widely used in dosimetry protocols to calculate  $P_{\text{wall}}$  corrections, it deserves further study.

## ACKNOWLEDGMENTS

We wish to thank our colleagues Ernesto Mainegra-Hing, Malcolm McEwen, Carl Ross, and Patrick Saull at the NRCC and Alan Nahum at the Fox Chase Cancer Center for their helpful comments regarding this paper. L.B. also wishes to acknowledge support from the Natural Sciences and Engineering Research Council of Canada.

- <sup>a)</sup>Also at: Physics Department, Carleton University, Ottawa, K1S 5B6, Canada; electronic mail: lbuckley@irs.phy.nrc.ca
- <sup>1</sup>AAPM TG-21, "A protocol for the determination of absorbed dose from high-energy photon and electron beams," *Med. Phys.* **10**, 741–771 (1983).
- <sup>2</sup>P. R. Almond, P. J. Biggs, B. M. Coursey, W. F. Hanson, M. S. Huq, R. Nath, and D. W. O. Rogers, "AAPM's TG-51 protocol for clinical reference dosimetry of high-energy photon and electron beams," *Med. Phys.* **26**, 1847–1870 (1999).
- <sup>3</sup>IAEA, *Absorbed Dose Determination in External Beam Radiotherapy: An International Code of Practice for Dosimetry Based on Standards of Absorbed Dose to Water*, Technical Report Series, Vol. 398 (IAEA, Vienna, 2001).
- <sup>4</sup>M.-T. Niatel, T. P. Loftus, and W. Oetzmann, "Comparison of exposure standards for <sup>60</sup>Co Gamma rays," *Metrologia* **11**, 17–23 (1975).
- <sup>5</sup>P. R. Almond and H. Svensson, "Ionization chamber dosimetry for photon and electron beams," *Acta Radiol.: Ther., Phys., Biol.* **16**, 177–186 (1977).
- <sup>6</sup>I. Kawrakow, "Accurate condensed history Monte Carlo simulation of electron transport. I. EGSnrc, The new EGS4 version," *Med. Phys.* **27**, 485–498 (2000).
- <sup>7</sup>I. Kawrakow and D. W. O. Rogers, "The EGSnrc Code System: Monte Carlo simulation of electron and photon transport," Technical Report No. PIRS-701, National Research Council of Canada, Ottawa, Canada (2000), see <http://www.irs.inms.nrc.ca/inms/irs/EGSnrc/EGSnrc.html>.
- <sup>8</sup>I. Kawrakow, "Accurate condensed history Monte Carlo simulation of electron transport. II. Application to ion chamber response simulations," *Med. Phys.* **27**, 499–513 (2000).
- <sup>9</sup>A. E. Nahum, W. H. Henry, and C. K. Ross, "Response of carbon and aluminium walled thimble chamber in <sup>60</sup>Co and 20 MeV electron beams," *Proceedings of the Seventh International Conference on Medical Physics in Medical and Biological Engineering and Computing*, 1985, Vol. 23, pp. 612 and 613.
- <sup>10</sup>D. W. O. Rogers, I. Kawrakow, J. P. Seuntjens, and B. R. B. Walters, "NRC User Codes for EGSnrc," Technical Report No. PIRS-702, National Research Council of Canada, Ottawa, Canada (2000), see <http://www.irs.inms.nrc.ca/inms/irs/EGSnrc/EGSnrc.html>.
- <sup>11</sup>J. Borg, I. Kawrakow, D. W. O. Rogers, and J. P. Seuntjens, "Monte Carlo study of correction factors for Spencer-Attix cavity theory at photon energies at or above 100 keV," *Med. Phys.* **27**, 1804–1813 (2000).
- <sup>12</sup>D. W. O. Rogers, "Fundamentals of high energy x-ray and electron dosimetry protocols," in *Advances in Radiation Oncology Physics*, Medical Physics Monograph Vol. 19, edited by J. Purdy (AAPM, New York, 1992), pp. 181–223.
- <sup>13</sup>A. F. Bielajew and D. W. O. Rogers, "Implications of new correction factors on primary air kerma standards in <sup>60</sup>Co beams," *Phys. Med. Biol.* **37**, 1283–1291 (1992).
- <sup>14</sup>ICRU, "Stopping powers for electrons and positrons," ICRU Report No. 37, ICRU, Washington, DC, 1984.
- <sup>15</sup>H. Bichsel and T. Hiraoka, "Energy loss of 70 MeV protons in elements," *Nucl. Instrum. Methods Phys. Res. B* **66**, 345–351 (1992).
- <sup>16</sup>M. S. MacPherson, "PhD Thesis: Accurate Measurements of the Collision Stopping Powers for 5 to 30 MeV Electrons," NRC Report No. PIRS 626, 1998.
- <sup>17</sup>M. S. MacPherson, C. K. Ross, and D. W. O. Rogers, "Measured electron stopping powers for elemental absorbers," *Med. Phys.* **23**, 797 (1996).
- <sup>18</sup>IAEA, *Absorbed Dose Determination in Photon and Electron Beams; An International Code of Practice*, Technical Report Series Vol. 277 (IAEA, Vienna, 1987).
- <sup>19</sup>G. D. Lempert, R. Nath, and R. J. Schulz, "Fraction of ionization from electrons arising in the wall of an ionization chamber," *Med. Phys.* **10**, 1–3 (1983).
- <sup>20</sup>D. W. O. Rogers and A. Booth, "PROT: A general purpose utility for calculating quantities related to dosimetry protocols," Technical Report No. PIRS-529 (rev. in preparation), NRC Canada, Ottawa, K1A 0R6, 2003.
- <sup>21</sup>G. Mora, A. Maio, and D. W. O. Rogers, "Monte Carlo simulation of a typical <sup>60</sup>Co therapy source," *Med. Phys.* **26**, 2494–2502 (1999).
- <sup>22</sup>I. Kawrakow and M. Fippel, "Investigation of variance reduction techniques for Monte Carlo photon dose calculation using XVMC," *Phys. Med. Biol.* **45**, 2163–2184 (2000).
- <sup>23</sup>E. Mainegra-Hing, I. Kawrakow, and D. W. O. Rogers, "Calculations for plane-parallel ion chambers in <sup>60</sup>Co beams using the EGSnrc Monte Carlo code," *Med. Phys.* **30**, 179–189 (2003).
- <sup>24</sup>C.-M. Ma and A. E. Nahum, "Effect of size and composition of central electrode on the response of cylindrical ionisation chambers in high-energy photon and electron beams," *Phys. Med. Biol.* **38**, 267–290 (1993).
- <sup>25</sup>A. Palm and O. Mattsson, "Experimental study on the influence of the central electrode in Farmer-type ionization chambers," *Phys. Med. Biol.* **44**, 1299–1308 (1999).
- <sup>26</sup>J. H. Hubbell, "Photon mass attenuation and energy-absorption coefficients from 1 keV to 20 MeV," *Int. J. Appl. Radiat. Isot.* **33**, 1269–1290 (1982).
- <sup>27</sup>S. M. Seltzer, "Calculation of photon mass energy-transfer and mass energy-absorption coefficients (dosimetry application)," *Radiat. Res.* **136**, 147–170 (1993).
- <sup>28</sup>J. H. Hubbell and S. M. Seltzer, "Tables of x-ray mass attenuation coefficients and mass energy-absorption coefficients 1 keV to 20 MeV for elements Z=1 to 92 and 48 additional substances of dosimetric interest," Technical Report No. NISTIR 5632, NIST, Gaithersburg, MD 20899, 1995.